THE CREEP DESIGN OF THIN PRESSURE VESSEL END CLOSURES

A.M. GOODMAN

Central Electricity Generating Board,
Berkeley Nuclear Laboratories, Berkeley, Gloucestershire GL 13 9PB, United Kingdom

SUMMARY

Recent analytical work on the creep of structures has paid increasing attention to concepts of creep damage. Locally severe creep damage will give rise to an enhanced (tertiary) creep rate for a given stress, leading to further load-shedding and delaying rupture. Simplified design methods can be proposed assuming this behaviour.

For infinite ductility, failure will be by collapse as a mechanism. However, generating plant components are intended for long lives, when a limited material ductility must be considered. Also, for thin pressure parts, the further stress redistribution is greatly restricted by the need to satisfy equilibrium, resulting in high tertiary strain rates.

The problem is investigated for the torispherical closure, using computer analyses which include the effects of tertiary creep and shape changes. The results are compared with the predictions of approximate methods, for which suitable adjustments are suggested. Changes of shape are shown to be advantageous.

1. Introduction

The majority of reported analytical work on the creep of structures has assumed that a simple constitutive relation, containing constant coefficients and exponents, is a sufficient representation of the material behaviour [1-3]. Until recently, such calculations were stopped at a close approach to the stationary stress state, and did not consider the later effect on the distributions of stress and strain when the material is locally weakened by accumulated creep damage. The omission has been shown to lead to undue pessimism in design [4-5].

This paper considers the consequences of locally severe material damage and tertiary creep. The most highly stressed part of the structure will enter tertiary creep first, when the local increases in strain rates will introduce a second period of stress redistribution and relaxation. At the reduced stress, further damage will accumulate more slowly than at the original stress and creep rupture will be delayed.

If material ductility is "infinite", i.e. greater than about 10% [5], the failure mode envisaged is analogous to plastic collapse, the structure deforming as a mechanism when sufficient of the material is in tertiary. Goodall and Cockroft [4] have shown that this leads to an upper bound assessment of the life of the component. In a later paper [5], Goodall, Cockroft and Chubb have shown that this life is closely approached by some real structures.

The useful life will in practice be limited by the available ductility in tertiary creep and by any restrictions on stress redistribution. Thick structures have more redundant material at discontinuities than thin pressure vessels. For the latter, while some reduction in peak stress levels due to tertiary creep would be expected, these stresses must stabilise again if the internal pressure is to be contained. Strain rates will then accelerate, placing greater demands on material ductility. For a thin shell structure, excessive finite deformation may be a further limitation.

Computer analyses are used here to examine these limitations for the case of the torispherical end closure. In order to quantify strains and deformations a reasonably realistic constitutive relation is used with the inclusion of tertiary creep. Small strain theory restricts attempts to continue this realism to failure. However, it is considered that there is a useful correlation between this restriction and the material ductility found in tests lasting $\sim 10^5$ hours, since both are about 5%.

In view of the demands made on the most modern computers by analyses involving tertiary creep, the development of simpler methods for design or design assessment is of paramount importance. An objective of this research has been to demonstrate the reliability of such methods applied to a thin pressure vessel.

2. Range of Vessels Examined

The geometric parameters for the range of vessel shapes considered are summarised in Table 1, in terms of the usual dimensionless quantities h/D, r/D and t/D (Figure 1). Geometries 1 through 4 represent limiting combinations of h/D and t/D. Geometry 4 (deep, thick) was considered to be of reduced practical importance and was excluded from the detailed calculations. Geometries 5 and 6 represent a more typical depth of dishing

(h/D = 0.22), with the same limiting values of t/D.

Table 1 also lists the computed elastic and elastic/perfectly plastic stress concentration factors (S.C.F's) due to uniform internal pressure loading. The computations were performed using the C.E.G.B. program PATAS [6]. The criterion of plastic collapse was that of Townley et al [7], that is a maximum plastic strain in excess of 1%. The normalising stress σ_o^* is the von Mises equivalent stress which would obtain in the membrane region of a drum of the same thickness as the end closure. Elastic modulus, Poisson's ratio and yield stress are typical values for a mild steel ($E = 2.07 \times 10^5$ [MN/m^2], $\nu = 0.3$, $\sigma_y = 207$ [MN/m^2]).

3. Representation of Creep

3.1 Primary and Secondary Creep

Typical curves of creep strain against time, as might be obtained from a uniaxial constant stress test, are shown in Figure 2. A two-term mathematical formulation, in a form due to Marin and McVetty [8, 9], has been used to describe fast primary and linear secondary creep:

$$\varepsilon_c = \alpha_1 \left(\frac{\sigma}{\sigma_o}\right)^{\eta_1} (1 - e^{-qt}) + \alpha_2 \left(\frac{\sigma}{\sigma_o}\right)^{\eta_2} t \qquad \ldots(1)$$

Reliable medium-term high sensitivity strain data for 0.19% carbon steel at 450°C have been made available by Skelton and Crossland [10]. In fitting these data, it was found necessary to allow η_2 to vary in a linear manner with stress (Figure 3). The numerical values for the parameters are summarised below (S.I. units, time in hours):

$$\alpha_1 = 0.43 \times 10^{-3} \qquad \alpha_2 = 0.125 \times 10^{-6} \qquad \eta_1 = 4.47 \qquad q = 0.017$$

$$\eta_2 = 0.908 + 2.42 \frac{\sigma}{\sigma_o}$$

Here, σ_o is a normalising stress of 100 MN/m^2 introduced for computational convenience.

Relation (1) is normally differentiated for varying stress assuming that the terms describing primary and secondary creep components can be treated as separable:

$$\dot{\varepsilon}_c = q \left(\alpha_1 \left(\frac{\sigma}{\sigma_o}\right)^{\eta_1} - \varepsilon_{c1}\right) + \alpha_2 \left(\frac{\sigma}{\sigma_o}\right)^{\eta_2} \qquad \ldots(2)$$

This is a strain hardening formulation.

The source data covered a stress range of 93 MN/m^2 to 209 MN/m^2, extending out to 4000 hours. This was considered sufficient to determine secondary strain rates, and such trends of material behaviour as the variation of η_2 with stress. Instantaneous plastic strains have been removed from the data.

3.2 Extension to Include Tertiary Creep

The relation between time to rupture t_r, and constant stress, σ_r, is well represented for most steels over a limited stress range by:

$$t_r \cdot (\sigma_r)^{\chi} = C \qquad \ldots(3)$$

Suitable constants for this steel at 450°C were found to be,

$$C = 0.529 \times 10^{16} \qquad \chi = 5.43$$

In the absence of better long term data, it has been assumed that the exponent χ is constant for all rupture times t_r.

The damage sum, λ_σ, given by

$$\lambda_\sigma = \int \frac{dt}{t_r(\sigma)} \qquad \ldots(4)$$

for varying stress, can be readily incorporated into computer calculations and output. This has the characteristic that the damage is unity at rupture, when the tertiary creep rate of a ductile material approaches infinity. A realistic representation of tertiary creep, ε_{c3}, (Figure 2), might take the form,

$$\dot{\varepsilon}_{c3} = f(\sigma, \int \frac{dt}{t_r(\sigma)}) \qquad \ldots(5)$$

Kachanov [11] has suggested such a modification of the linear secondary creep term to produce the tertiary creep characteristic, as

$$\dot{\varepsilon}_{c3} = \dot{\varepsilon}_{c2} \cdot \frac{1}{1 - (\lambda_\sigma)^\phi} \qquad \ldots(6)$$

No further physical significance is attached to this formulation within this paper.

Combining (6) and (2),

$$\dot{\varepsilon}_c = q \left(\alpha_1 \left(\frac{\sigma}{\sigma_o} \right)^{\eta_1} - \varepsilon_{c1} \right) + \frac{\alpha_2 \left(\frac{\sigma}{\sigma_o} \right)^{\eta_2}}{1 - (\lambda_\sigma)^\phi} \qquad \ldots(7)$$

The exponent ϕ determines the shape of the tertiary curve; a comparison with the curves of Skelton and Crossland for the assumed value of $\phi = 5.0$ is shown in Figure 4.

Relation (7) predicts very reasonable characteristics at long times. Secondary creep is linear, the tertiary creep fits the rupture curve, while the linear secondary component of creep at rupture is nearly constant at 1% (Figure 5). This last characteristic is typical of mild and low alloy steels, as is shown by the correlations of Murphy [12].

3.3 Application to Multiaxially Stressed Structures

The computer calculations use the Prandtl-Reuss flow rules in conjunction with von Mises equivalent stresses. Their continuation towards failure using equation (7) implies the assumption of a Mises rupture surface. The shape of the creep rupture surface for multiaxial stress conditions is debatable [13]; available information suggests that a Mises ellipse is reasonable in the tension-tension quadrant of a biaxial stress space and conservative in other quadrants.

Present information suggests that tertiary creep and rupture are inhibited or delayed by a compressive hydrostatic stress [14]. No correction for this has been made in the analyses, but the effect is considered when the results are interpreted. Possible non-zero volumetric strains due to void formation have been assumed to be negligibly small.

No realism is claimed for the calculated stresses and strains in heavily damaged areas when the equivalent strain exceeds the 5% limit. However, the material is then so weak that it is not considered to make any further significant contribution to the overall behaviour

of the structure.

4. Approximate Methods of Creep Analysis

Although a powerful analytical tool, the use of a modern computer program requires some experience for reliable application and can be expensive if the problem is non-linear. The latter is particularly true for complex structures in tertiary creep. Approximate methods have been proposed to simplify the design procedure, and one objective of this research is to examine the applicability of such simple design methods to a thin pressure vessel.

A number of potentially suitable techniques have been developed in recent years; these consider established characteristics of structural behaviour in plasticity and creep, but do not require non-linear computer analyses for their application. It is first considered that the material strength with stress in creep is determined by a constant exponent, n:

$$\varepsilon_c = A\sigma^n f(t), \qquad \ldots(8)$$

where A is a constant.

It has been observed (see [15]) that for a wide range of structures, the relaxed stationary state S.C.F. for a stress index of n, Γ^n, is inversely proportional to n. $\Gamma^{n=1}$ gives the elastic S.C.F., while analogy can be made between $\Gamma^{n\to\infty}$ and the perfectly-plastic S.C.F.

By proportion,

$$\Gamma^n = \Gamma^{n\to\infty}\left(1 + \frac{1}{n}(\psi - 1)\right) \qquad \ldots(9)$$

where $\psi = \Gamma^{n=1}/\Gamma^{n\to\infty}$

If the normalising stress remains proportional to the applied pressure load P,

$$\Gamma^{n=1} = \frac{\sigma_y}{P_y}$$

where P_y is the load to cause the first point in the structure to yield for a material of any yield stress σ_y. For the perfectly plastic material,

$$\Gamma^{n\to\infty} = \frac{\sigma_y}{P_u},$$

Where P_u is the collapse load.

Then,

$$\bar{\bar{\sigma}} = P\Gamma^{n\to\infty} = \frac{P\sigma_y}{P_u} \qquad \ldots(10)$$

$$\bar{\sigma} = P\Gamma^n = \frac{P\sigma_y}{P_u}\left(1 + \frac{1}{n}\left(\frac{P_u}{P_y} - 1\right)\right) \qquad \ldots(11)$$

The quantities $\bar{\sigma}$ and $\bar{\bar{\sigma}}$ are common to many of the more recent approximate methods of design. They can be obtained from a combination of elastic and limit load analyses of any structure.

The reference stress method has been proposed as an assessment of structural deformation in creep (see [16]). It is assumed that the time dependent deformation is proportional

to the time dependent strain at the reference stress, $\sigma_{ref.}$, for any time t:

$$\frac{\Delta h_c(t)}{\Delta h_E} = \left(\frac{\epsilon_c(t)}{\epsilon_E}\right)_{\sigma_{ref.}}, \qquad \ldots(12)$$

Where $\Delta h_c(t)$ is time dependent deformation,

Δh_E is the elastic deformation of the same point on the component,

$\epsilon_c(t)$ is the uniaxial creep strain at time t and stress $\sigma_{ref.}$,

ϵ_E is the uniaxial elastic strain at stress $\sigma_{ref.}$

The insensitivity of the reference stress to n has been invoked by Sim [17] to obtain,

$$\sigma_{ref.} = \bar{\bar{\sigma}} = \frac{P\sigma_y}{P_u} \qquad \ldots(13)$$

Ponter and Leckie [18] have shown that this is an upper bound to the reference stress during secondary creep.

Goodall and Cockroft [4] have described upper and lower bounds to the life of a structure in creep. The lower bound expects rupture when the first point in the structure enters tertiary creep. Assuming the applicability of equation (3), then the lower bound rupture time, $\bar{t}_r$, is given by:

$$\bar{t}_r = C(\bar{\sigma})^{-\chi} \qquad \ldots(14)$$

The upper bound has been discussed in the Introduction; creep deformation is predicted to become unbounded at a time $\bar{\bar{t}}_r$ given by:

$$\bar{\bar{t}}_r = C(\bar{\bar{\sigma}})^{-\chi} = C\left(\frac{P\sigma_y}{P_u}\right)^{-\chi} \qquad \ldots(15)$$

This is also the time to rupture read from the t_r, σ_r curve at reference stress level, for similar deformation and creep failure surfaces.

5. Results

5.1 Results of Computation

The analyses assumed constant internal pressure loading. Design of the torispheres was notional, intended only to give creep lives of the same order as components in the power generation industry. An initial estimate of endurance was taken as the time to 1% creep at the maximum elastic stress divided by 1.5. Table 2 lists the pressure loads, these initial life estimates and the quantity $\bar{\bar{\sigma}}$ in dimensional form.

Figures 6 through 10 summarise the computed results. Four variables are presented for each geometry; the deflection at the pole, $\Delta h/D$, together with the von Mises stress and strain and the damage sum λ_σ for the point of maximum initial stress. It was found that this remained the location of maximum damage and maximum creep strain throughout a small deformation analysis.

The computations describe a second period of stress redistribution due to tertiary creep, when load is shed from damaged material to surrounding material which is stronger in

creep. The reduction in the peak stress is greater than during the first period of relaxation due to primary creep.

Tertiary creep does not immediately increase the strain rate. This suggests that some local kinematic determinacy is maintained. The reducing peak stress tends to a nearly stationary value if computation is continued, as is necessary to satisfy equilibrium. As the stress levels out, the strain rate then increases rapidly.

For the analyses restricted by small strain theory and ductility considerations, the deflection at the pole is only slightly affected by the confined areas of damaged material. The predicted deflections from reference stress theory show noteworthy agreement with the computed results.

The elastic plastic analysis showed that geometry 2 would be limited at low temperatures by plastic ballooning of the drum. High temperature calculations including tertiary creep showed analagous behaviour, which could be seen in the computer output as indefinitely increasing circumferential strain in the cylindrical section.

The analysis of geometry 5 was continued to the closest approach possible to collapse of the vessel, accepting for the purpose any doubt about the use of small strain theory. The results are shown in Figure 11. The failure asymptote at $0.48\ \bar{t}_r$, although nearer the upper than the lower bound, still falls somewhat short.

The maximum compressive hydrostatic stress was found to occur on the outer surface, opposite the peak equivalent stress location on the inside. The probable delay in tertiary creep due to hydrostatic compression has not been modelled in these analyses. Figure 13 shows that the outer surface still does not enter tertiary until a late stage in the computation; it is considered that the lack of this detail is unimportant.

5.2 Estimates of Creep Endurance

Table 3 lists the life estimates for the vessels according to various calculations and design limits. The figures have been normalised against a computed estimate for each geometry. This is taken to be the computed behaviour prediction, including tertiary creep, with a ductility limit of 5% maximum creep strain. The elastic estimate is included for its similarity to an assessment of a typical design code approach, and reference stress theory has been used to predict an endurance with excessive bounded deformation, taken to be $\Delta h/D \geq 0.05$ as the design limit.

Apart from the elastic calculation, all the estimates for geometry 2 are the same. Otherwise, it is found that the upper bound prediction of collapse and the deformation assessment are optimistic, while the lower bound and elastic estimates of rupture time are pessimistic. The deformation criterion is nowhere limiting.

5.3 Effect of Shape Changes

The computations for geometries 3 and 5 were repeated with allowance made for axisymmetric changes of shape, including thinning of the section due to plastic strains. The results have been superimposed on Figures 8 and 9. In both cases, the vessel deforms to a better shape to accommodate the internal pressure. The peak stress reduces continuously, while material damage, creep strain and deformation all accumulate less rapidly.

6. Discussion

The continued analysis of geometry 5, during which strains of more than 20% were calculated, showed a failure asymptote for this vessel at only 48% of the endurance predicted by the upper bound theorem. A similar result has been found for beams subjected to bending and end load and allowed infinite ductility [19]. Since different materials are assumed, a comparison in terms of predicted life is difficult. An approximate formula in terms of load carrying capacity has been suggested [5]:

$$\frac{\bar{P}}{P} = 1 + 0.05 \left(\frac{P_u}{P_y} - 1\right) \qquad \ldots(16)$$

where P is the actual load, $\bar{P}$ that given by upper bound analysis. This formula is optimistic by about 7% on load for both the beams and the torispheres. A change in the adjustment factor from 0.05 to 0.10 is suggested to ensure conservatism, particularly for the less restrained structures considered here.

A mechanical explanation can be postulated. Figures 6 to 10 show that the freedom of damaged material to off-load is limited, most probably by the need to maintain equilibrium, and that beyond this limit strain and deformation rates increase. For both beams and thin vessels initially plane sections are constrained to remain plane by the requirements of compatibility. This is a restraint on the variability of strain rate through a section not found in thicker structures, which may be expected to inhibit stress redistribution.

A consideration of the stress categories, defined in ASME Codes 1331/8 and 1592, is helpful. Where only membrane stresses exist, these are statically determined and it is known that the upper bound coincides with the lower bound. This applies to the drum of geometry 2. Where the structure contains local discontinuity stresses the results of [5] show that the upper bound endurance is closely approached. The beams and torispheres contain membrane and bending stresses only, and the intermediate result is seen.

Where the bounds are widely separated, a more real limitation, in design for the long lives required by the power generation industry, is the limited ductility shown by most steels after long exposure to creep. A maximum local von Mises strain of 5% has been assumed as a reasonable limit in this paper. Comparing column E with columns A to D in Table 3, it is found that only the predictions of the bounds of reference [4] bear consistent relationships to the computed endurance assessments. For example, the lower bound estimate, except for the special case of geometry 2, is always about one-third of the computed estimate.

Such a relation to the lower bound is physically reasonable. For any given ratio between a material ductility limit and the strain at the onset of tertiary, there will be a corresponding ratio between the time to failure and the lower bound rupture time. The non-linear behaviour due to tertiary creep is such that the second ratio will be lower than the first. However, these results and those of reference [5] show that kinematic determinacy of a complex structure slows this departure from linearity. Consequently, the two ratios will be more nearly equal, and less dependent on structure geometry, than might be expected from uniaxial test curves. Here, the assumed ductility ratio is 5.0, the failure time ratio nearly constant at 3.0, comparing columns F and E of Table 3.

These observations suggest a simple method of design assessment where limited ductility must be considered. For a ductility ratio, $\varepsilon_f/\bar{\varepsilon} = 5.0$, these results show that a failure time ratio, t_f/t_r, given by,

$$\frac{t_f}{t_r} = 1.0 + 0.5\left(\frac{\varepsilon_f}{\bar{\varepsilon}} - 1.0\right) \qquad \ldots(17)$$

is reasonable for the torisphere. Since non-linearity increases with time, this will be conservative for all smaller ductility ratios.

Any assessment must also be subject to the condition that the upper bound collapse time is not exceeded. The two step procedure that is indicated takes the lesser of t_{f1} and t_{f2}, where

$$t_{f1} = \bar{t}_r \cdot \left[1.0 + 0.5\left(\frac{\varepsilon_f}{\bar{\varepsilon}} - 1.0\right)\right]$$

and $$t_{f2} = \bar{\bar{t}}_r \cdot \left[1.0 + 0.10\left(\frac{P_u}{P_y} - 1.0\right)\right]^{-\chi} \qquad \ldots(18)$$

Further data are necessary before such a principle could be extended to cover other materials, particularly the austenitic steels, or other vessel geometries. Where the ductility ratio is greater than about 5.0, increasing non-linearity will make this philosophy more difficult to apply, although the creep ductile endurance would now be closely approached.

7. Conclusions

(i) Predictions of deformation using the "Reference Stress" technique have been found to be reasonable for a thin pressure vessel during secondary creep.

(ii) No evidence was found that the creep design of thin torispheres might be limited by excessive bounded deformation.

(iii) A suitable adjustment has been suggested to an existing approximate formula for the creep ductile load carrying capacity of structures, which ensures conservatism for less restrained components, such as the torispherical end closure.

(iv) Where a limit is applied to the material ductility, these results have shown that the failure time can be simply related to the brittle creep rupture time and the material ductility ratio.

(v) For these torispheres, shape changes due to pressure loading offer a further conservatism.

Acknowledgement

This paper is published by permission of the Central Electricity Generating Board.

References

[1] PENNY, R.K., "The Creep of Spherical Shells Containing Discontinuities", Int. J. Mech. Sci., 9, 1967, 373-388.

[2] MURAKAMI, S. and IWATSUKI, S., "Transient Creep of Circular Cylindrical Shells", Int. J. Mech. Sci., 11, 1969, 897-912.

[3] MURAKAMI, S. and YAMADA, Y., "Effects of Hydrostatic Pressure and Material Anisotropy on the Transient Creep of Thick Walled Tubes", Int. J. Mech. Sci., 16, 1974, 145-160.

[4] GOODALL, I.W. and COCKROFT, R.D.H., "On Bounding the Life of Structures Subjected to Steady Load and Operating within the Creep Range", Int. J. Mech. Sci., 15, 1973, 251-263.

[5] GOODALL, I.W., COCKROFT, R.D.H. and CHUBB, E.J., "An Approximate Description of the Creep Rupture of Structures", Int. J. Mech. Sci., To be published, 1975.

[6] GOODMAN, A.M., C.E.G.B. Report RD/B/N2584, 1973.

[7] TOWNLEY, C.H.A., FINDLAY, G.E., GOODMAN, A.M. and STANLEY, P., "Elastic-Plastic Computations as a Basis for Design Charts for Torispherical Pressure Vessel Ends", Proc. I. Mech. E., 185, 1971, 63.

[8] McVETTY, P.G., "Working Stresses for High Temperature Service", Mech. Eng., 56, 1934, 149.

[9] PAO, Y.K. and MARIN, J., "An Analytical Theory of the Creep Deformation of Metals", J. Appl. Mech., 20, 1953, 245.

[10] SKELTON, W.J. and CROSSLAND, B., "Results of High Sensitivity Tensile Creep Tests on a 0.19% Carbon Steel used for Thick-Walled Cylinder Creep Tests", Proc. I. Mech.E., 182, 1967, 151-158.

[11] KACHANOV, L.M., "Time to Failure under Creep Conditions", Izv. Akad. Nauk., U.S.S.R., Otd. Tekhn. Nauk., 8, 1958.

[12] MURPHY, M.C., "Rating the Creep Behaviour of Heat-Resistant Steels for Steam Power Plant", Metals Eng. Quart., 1973, 41-50.

[13] HAYHURST, D.R., "Creep Rupture under Multiaxial States of Stress", J. Mech. Phys. Solids, 20, 1972.

[14] DUTTON, R., "A Survey of Compression Creep Testing of Metals", Materials Research and Standards, April, 1969.

[15] CALLADINE, C.R., "Time Scales for Redistribution of Stress in Creep of Structures", Proc. Roy. Soc., A309, 1969, 363.

[16] PENNY, R.K. and MARRIOTT, D.L., "Design for Creep", McGraw Hill Book Co., 1971.

[17] SIM, R.G., Ph.D. Dissertation, Univ. of Cambridge, 1968.

[18] LECKIE, F.A. and PONTER, A.R.S., "Deformation Bounds for Bodies which Creep in the Plastic Range", J. Appl. Mech., 1970, 426-30.

[19] CHUBB, E.J., CEGB Report RD/B/N3370, 1975.

Head Geometry	See Figure 1 $\frac{h}{D}$	$\frac{t}{D}$	$\frac{r}{D}$	$\frac{\sigma_E^*}{\sigma_o^*}$	Location	$\frac{\sigma_{Pu}^*}{\sigma_o^*}$	Pu/Py $= \frac{\sigma_{Pu}^*}{\sigma_o^*}$
1	0.15	0.05	0.10	3.87	Crown	1.72	2.26
2	0.40	0.01	0.10	1.36	Knuckle	1.0(1)	1.37
3	0.15	0.01	0.10	6.75	Knuckle	2.82	2.39
5	0.22	0.01	0.10	3.42	Knuckle	1.57	2.18
6	0.22	0.05	0.10	2.26	Knuckle	1.03	2.26

TABLE 1 Geometry Parameters, Results of Elastic and Plastic Computations

Note: (1) Drum limiting

Head Geometry	Pressure Load MN/m^2	Initial Elastic Endurance Estimate (1) hours	Reference Stress, $= \bar{\sigma} = \frac{P_{\sigma y}}{P_u}$ MN/m^2
1	4.80	63,000	71.6
2	2.10	136,000	90.2
3	0.45	117,000	54.9
5	0.85	136,000	57.1
6	6.80	122,000	57.3

TABLE 2 Initial Elastic Endurance Estimate

Note: (1) Estimate based on elastic stress ÷ 1.5, time to 1% creep strain.

Head Geometry	Elastic Estimate (see Table 2)	Computed Lower Bound [4] $\bar{t}_r$	Upper Bound for Unlimited Ductility [4] $\bar{\bar{t}}_r$	Reference Stress, Distortion Limit (1) [16]	Computation Ductility Limit (2)	$3\bar{t}_r$ or Eq. (18)
	A	B	C	D	E	F
1	0.76	0.27	5.4	3.4	1.0	0.81
2	1.06	1.0(3)	1.0	1.0	1.0	1.0
3	0.35	0.34	5.7	1.2	1.0	1.01
5	0.38	0.35	4.3	2.7	1.0	1.06
6	0.51	0.38	6.3	3.5	1.0	1.13

TABLE 3 Comparison of Endurance Estimates

Notes: (1) Limit of 5% on Dh/D

(2) Limit of 5% on maximum equivalent creep strain

(3) Drum limiting

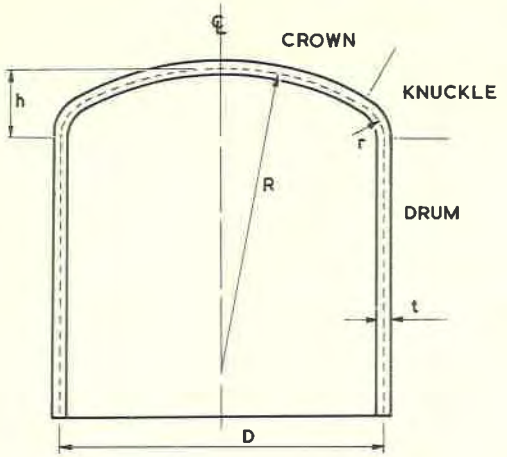

Fig. 1. Torispherical end closure on equal-thickness drum.

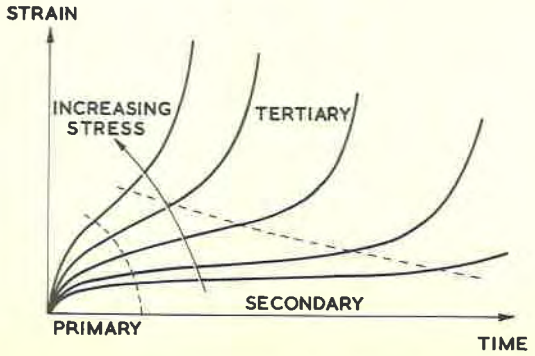

Fig. 2. Typical curves of creep strain against time for constant load.

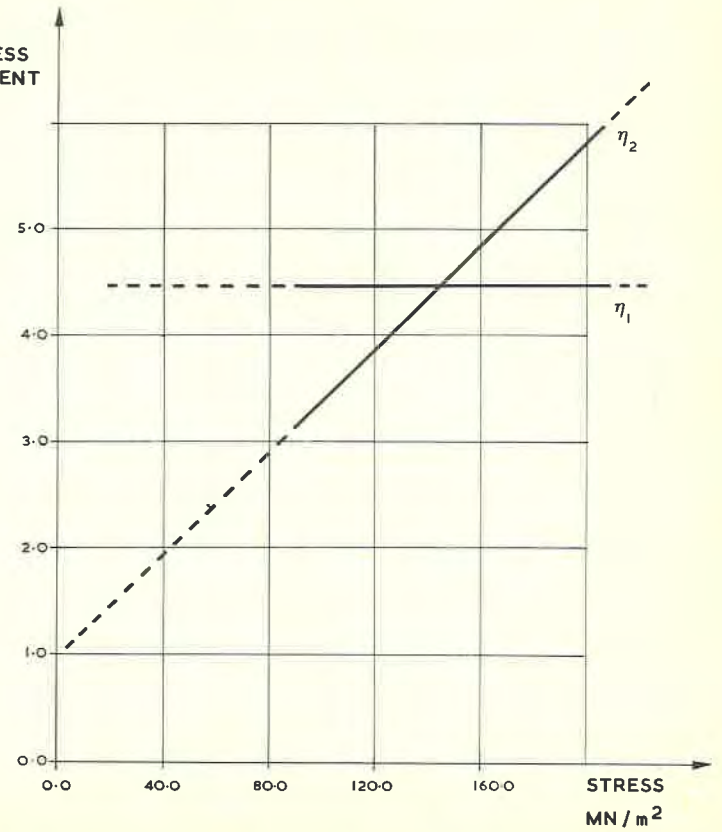

Fig. 3. Variations of exponents η_1 and η_2 with stress.

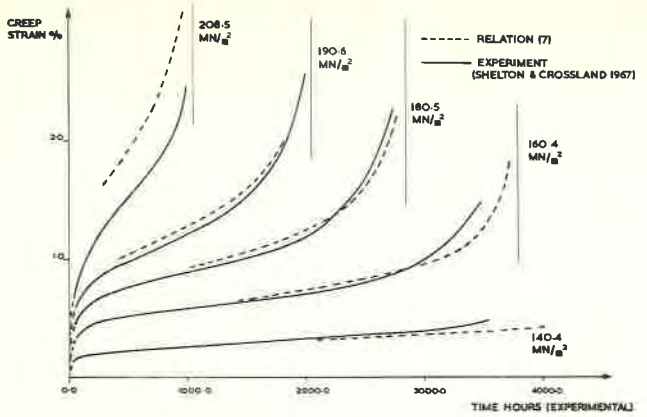

Fig. 4. Comparison of experimental data and fitted curves, time scale adjusted for scatter in experimental rupture.

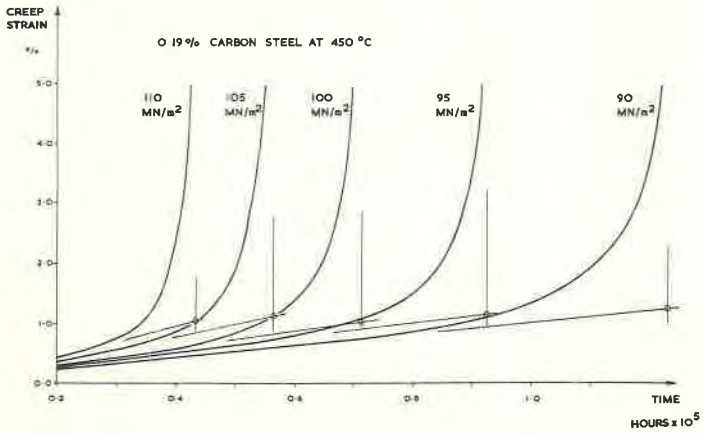

Fig. 5. Secondary component of creep at time to rupture.

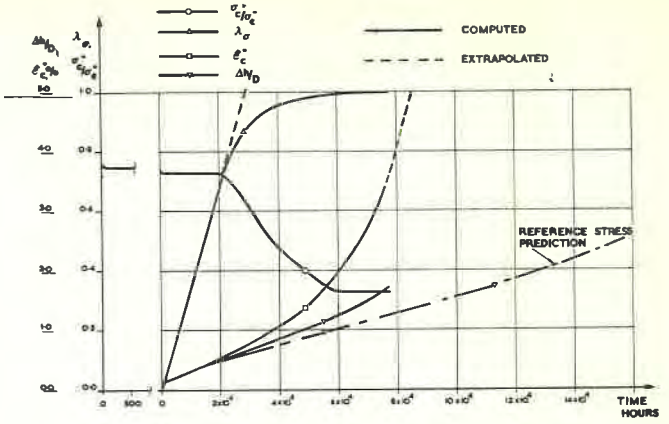

Fig. 6. Primary, secondary and tertiary creep behaviour of end closure, geometry 1.

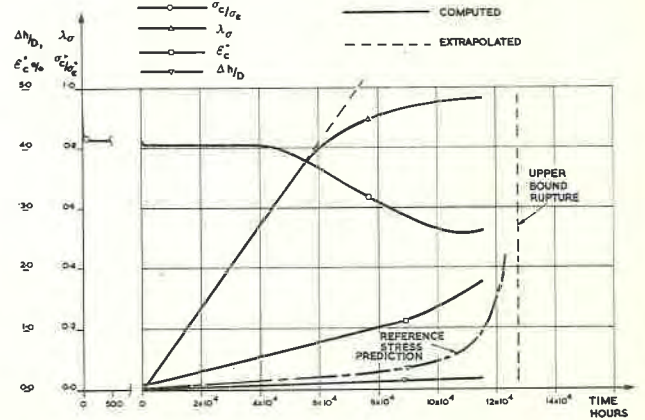

Fig. 7. Primary, secondary and tertiary creep behaviour of end closure, geometry 2.

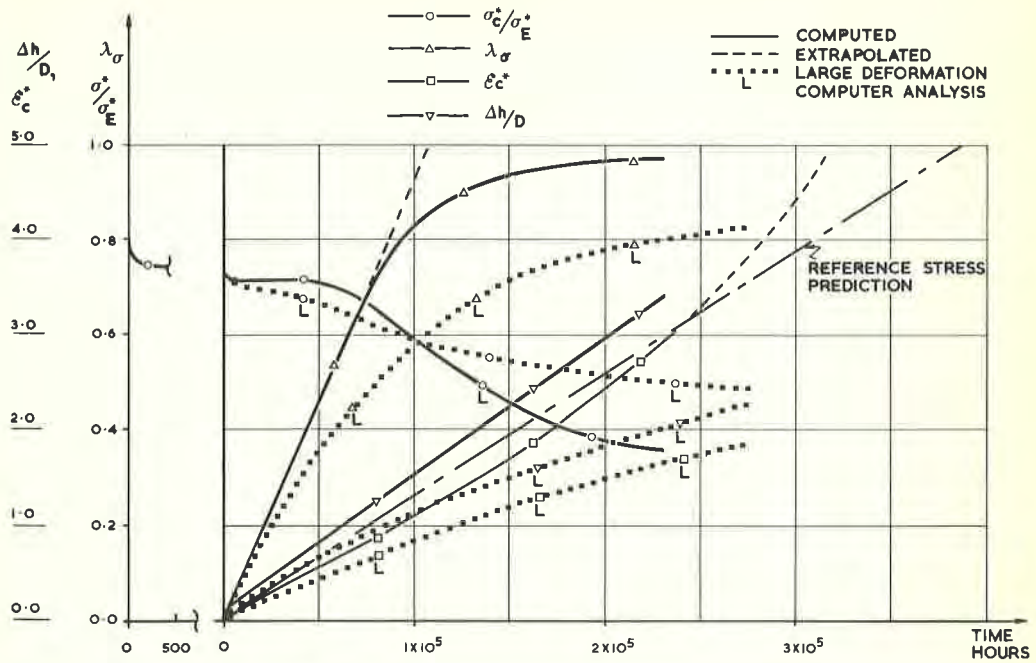

Fig. 8. Primary, secondary and tertiary creep behaviour of end closure, geometry 3.

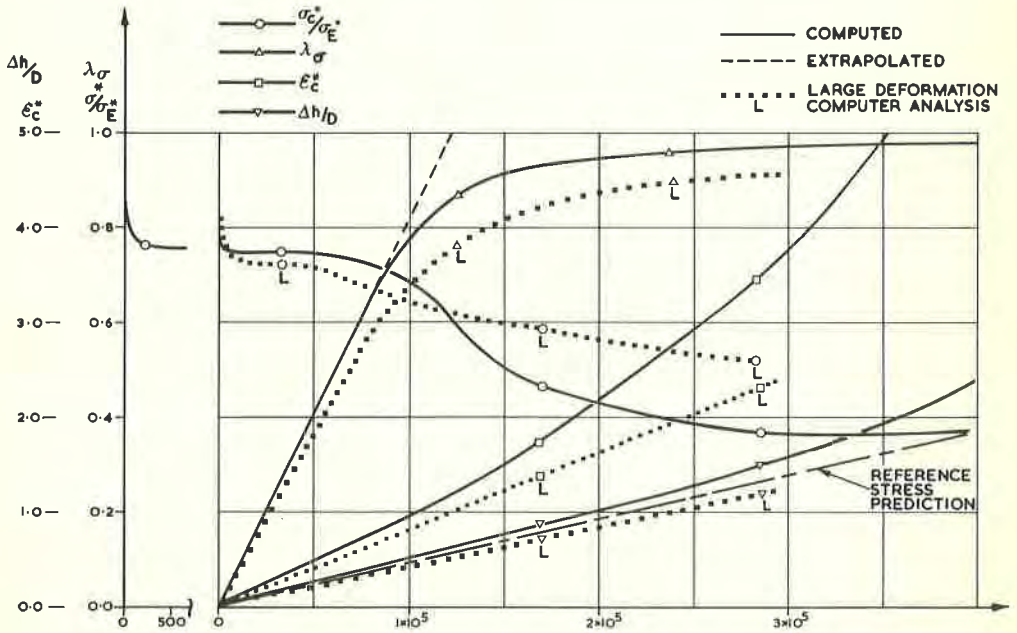

Fig. 9. Primary, secondary and tertiary creep behaviour of end closure, geometry 4.

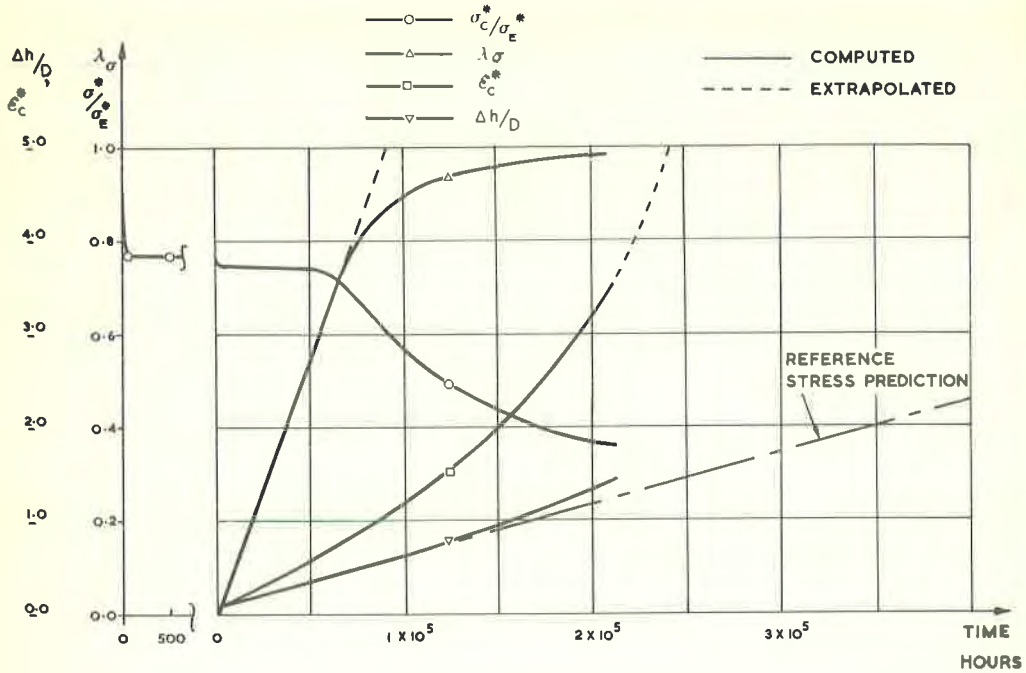

Fig. 10. Primary, secondary and tertiary creep behaviour of end closure, geometry 5.

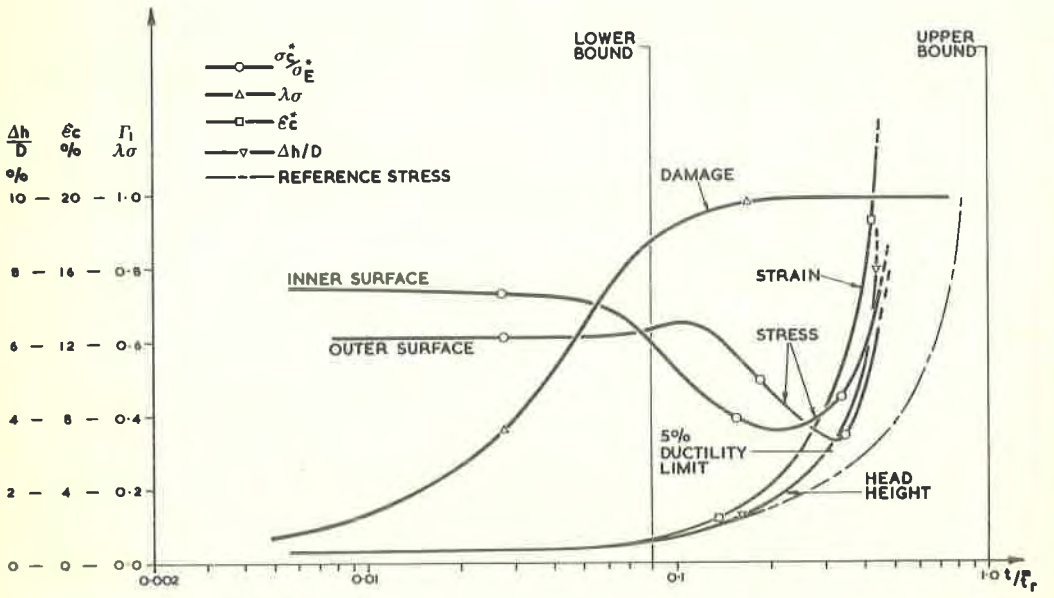

Fig. 11. Extended small strain analysis of geometry 5.